JOURNAL OF MATERIALS SCIENCE 4 (1969) 259-265

Conduction Processes in Vacuum-Deposited Films of Silicon Oxide

A. R. MORLEY*, D. S. CAMPBELL†, J. C. ANDERSON
Electrical Engineering Department, Imperial College, London SW7, UK

Received 22 September 1968

DC and AC conduction measurements were made on films of silicon oxide which had been fully annealed. Four activation energies were determined for the conduction processes. In the case of DC conduction a time-dependent absorption current was observed at low fields and this was related to a low-frequency dispersion. The steady-state current at low fields was ohmic. At high fields the conductivity was field-dependent and the usual $J \propto \exp(\beta V^{\frac{1}{2}})$ relationship was observed.

The low-frequency dispersion was found to affect the audio-frequency region at high temperatures. Above 10 kc/s the loss was independent of frequency up to 1 mc/s.

1. Introduction

Conduction processes in silicon oxide have been the subject of a number of publications [1-8]. However, the interpretation of similar results differs widely, mainly due to the uncertainties in the physical and energy band structure of the dielectric films.

DC conduction results can be considered in two distinct regions of low and high fields. Table I shows a simplified survey of some of the work already performed on silicon oxide. The low field region has received very little attention, probably due to the time-dependent nature of the current on initial application of the DC field. It is a general result, however, that the steady state current is ohmic but it is observed from table I that the explanations vary considerably. Hirose and Wada [2] and Argall [6] made use of the time-dependent current to show the presence of a low-frequency loss peak, using the analysis of Hamon [9].

The high-field region has already been discussed in a review by Jonscher [10] who showed that none of the proposed models fitted exactly the experimental results. The results of different authors agree reasonably well but they do not fit either straightforward Poole-Frenkel or Schottky emission type models. The model proposed by Simmons [11] required that for a $Al/SiO_x/Al$ sandwich, the Fermi level of the dielectric film was shifted to within less than 1 eV of the conduction band of the insulator. There is not sufficient information about the energy band structure of an amorphous dielectric to consider this model in any detail.

Table II gives a brief survey of some of the more important results from AC measurements on silicon oxide films. The most detailed analysis of the temperature and frequency behaviour of silicon oxide was performed by Argall [6]. He determined two low frequency peaks, with the type B peak affecting the audio-frequency conduction. Above the audio-frequency region the loss increased with frequency and Argall proposed an electronic hopping mechanism to explain the very low activation energy of 0.01 eV.

This paper reports an investigation of DC and AC conduction in films which have been prepared under similar deposition conditions and in particular those films which have been fully annealed. The heat-treatment of silicon oxide films to produce stable capacitors has been the subject of a previous paper [12]. An activation energy associated with the annealing process was found, but this is not related to electrical conduction in the film.

*Current address: Allen Clark Research Centre, The Plessey Company Limited, Caswell, Towcester, Northants.
†Visiting Senior Lecturer in Materials Science. Resident address: The Plessey Company Limited, Components Group, Whiteside Works, Bathgate, West Lothian, Scotland.

TABLE I Previous results on DC conduction.

Author	Low field properties	High field properties Activation energy	ϵ'_{se}*	Proposed mechanism
Hirose and Wada [2, 3]	$E = 0.37$eV, $= 5.10^{12}\,\Omega$ cm. Explained by diffusion of Si ions	0.54 eV	3	Poole-Frenkel conduction
Johansen [4]		0.56 eV	3.8	Schottky emission from small silicon islands into a silica matrix
Hartman, Blair and Bauer [5]	Ohmic	0.43 eV	3.0	Model proposed by O'Dwyer [24]
Stuart [7, 8]	Ohmic $E = 0.4$ eV	—	—	Model proposed by Simmons [11]
Argall [6]	Suggested that conductivity composed of both ionic and electronic contributions	—	—	—
Siddall [1]	Suggested that conductivity controlled by leakage paths	—	—	—

*This column gives the Schottky emission form of the permittivity ϵ'_{se} (see section 3.1.3).

TABLE II Previous results on AC conduction.

Author	Frequency range	Dispersions at room temp.	Activation energy	β*	γ_c ppm/°C	Reasons for dispersions	General behaviour
Argall [6]	10^{-2}–10^{7} c/s	Type A– 5×10^{-3} c/s Type B – 5×10^{-2} c/s	0.5 eV (10 Å /sec) 0.8 eV	A. $\beta = 0$ B. $\beta = 0.5$	220 (at 25° C mc/s)	A – short range movement of impurity ions B – blocking of charge carrier at electrodes	Over the audio-frequency range (100 c/s – 10 kc/s) tan$\delta\alpha$ $(\text{frequency})^{AI}$, where A is a constant and T is temperature. Above 100 kc/s, tan δ increases with frequency. This is explained in terms of electron hopping conduction with $E = 0.01$ eV.
Hirose and Wada [2]	10^{-2}–10^{7} c/s	lf 10^{-1} c/s hf $> 10^{7}$ c/s	0.36 eV —	$\beta > 0$ —	— —	lf diffusion of Si ions hf local torsional vibrations of SiO chains	—
Siddall [1]	Measured at 1 kc/s and 10 kc/s	—	—	—	100 for films deposited at < 5 Å/sec, 400 for those deposited at 10 Å /sec.	—	Ions initially controlled by leakage paths

*β, the distribution of relaxation times factor defined by Cole and Cole [14] (equation 4 in text).

2. Experimental

$Al/SiO_x/Al$ sandwiches were produced by evaporation from separate sources in one pump down cycle and measurements were performed with the capacitors remaining under vacuum. The silicon oxide was evaporated from a tantalum Drumheller type source [13] with the silicon oxide charge (supplied by the Kemet Company) in the central chimney. The pressure during the evaporation was 1×10^{-5} torr and a rate of 11 Å/sec. was controlled using a crystal rate monitor. The latter was also used to indicate the approximate

thickness (2000 Å). The actual rate was determined by measuring the thickness with a talysurf and monitoring the evaporation for a known time. Aluminium wire was evaporated from two tungsten spirals to a thickness of about 2000 Å for both bottom and top electrodes. The aluminium electrodes and the silicon oxide were deposited on to cleaned Corning-7059 glass substrates which were at room temperature prior to deposition. Temperatures were determined using a Cu/Ni thin-film thermocouple also deposited on to a Corning-7059 glass substrate. After alteration of temperature a period of 1.25 h was allowed for thermal equilibrium to be achieved.

DC measurements were made with a stabilised voltage supply and a type 610B Keithley electrometer. Audio-frequency measurements were made with a Wayne-Kerr B.211 bridge together with an Advance Signal generator and a Radiometer wave analyser. Radio-frequency measurements were made with an Airmec Signal generator and wave analyser together with a Wayne-Kerr B.601 bridge.

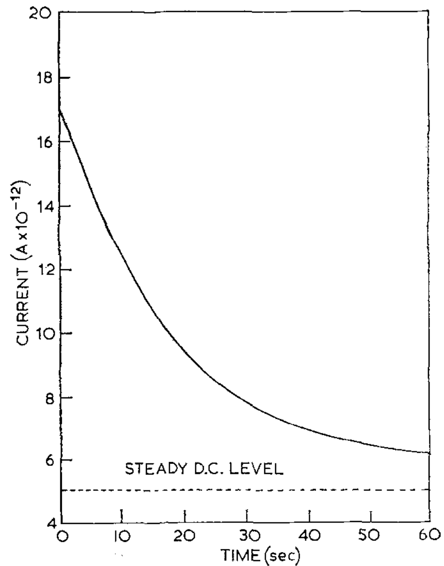

Figure 1 Decay of absorption current as a function of time, showing steady DC level.

3. Experimental Results

3.1. Conduction

3.1.1. Time-Dependent Current

For fields less than 0.05 mV/cm the application of a step voltage across a capacitor produced a current which decayed with time to a steady DC level. This absorption current behaviour is shown in fig. 1 for a field of 0.025 mV/cm. The steady DC level was obtained after applying the voltage for ½h. The change in current during the application of the voltage for a further ½ h was undetectable.

Hamon's equation [9] relates this absorption current $I(t)$ at a time t, to the dielectric loss (in terms of ϵ'') at a frequency f defined by $0.1/t$, thus;

$$\epsilon'' \simeq \frac{I(t)}{2\pi f C_a V}$$

where C_a is the capacitance with air as the dielectric and V is the applied voltage.

The result of performing the above transform is shown in fig. 2 in which ϵ'' is plotted in arbitrary units as a function of frequency. This plot indicates a low frequency loss peak in the region 5×10^{-3} c/s at room temperature.

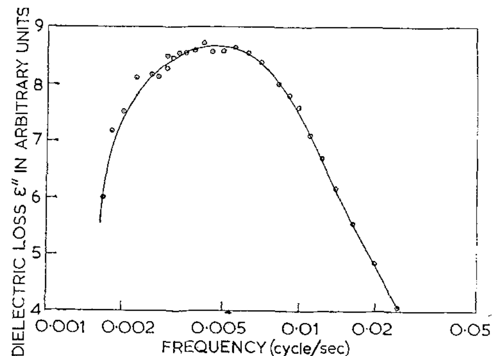

Figure 2 Dielectric loss, ϵ'' (calculated from absorption current) versus frequency.

3.1.2. Low Field Conduction

Current readings were taken 5 min after applying a step voltage so that the steady state DC level was very nearly attained. In between readings the capacitor was short-circuited for a similar period.

Low field conduction always gave an ohmic characteristic and a plot of log I versus log V is shown in fig. 3. The conductivity at room temperature is of the order $10^{-13}/\Omega$ cm. However this value varied by a few orders of magnitude for different capacitors prepared under the same deposition conditions and given identical heat-treatment.

An Arrhenius plot of conductivity versus

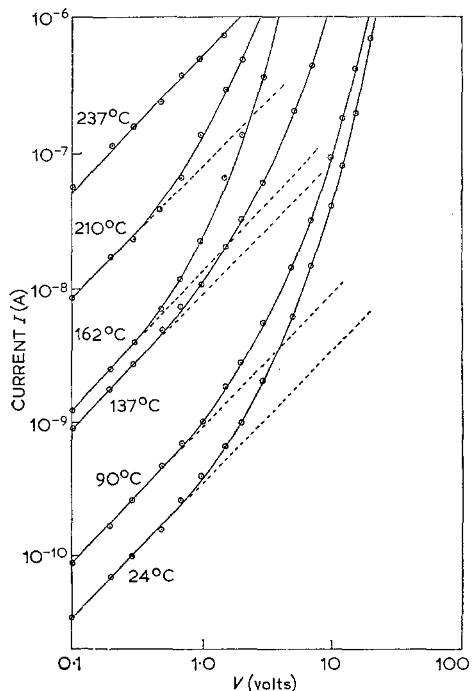

Figure 3 Current versus voltage at constant temperatures.

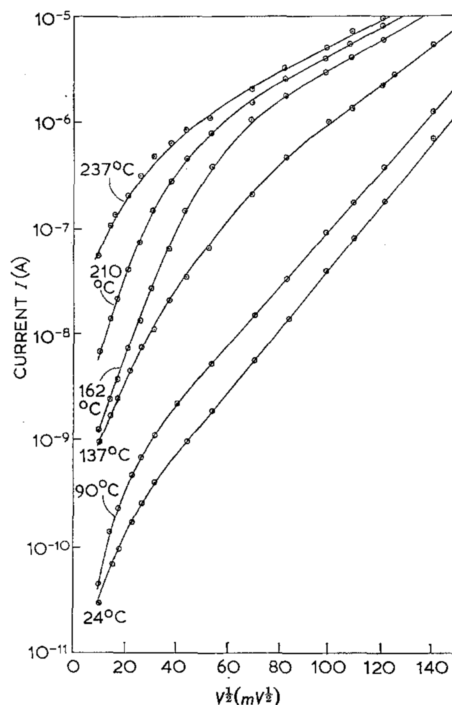

Figure 4 Log (current) versus (voltage)$^{\frac{1}{2}}$ at constant temperatures.

reciprocal temperature taken from fig. 3 gave an activation energy of 0.70 ± 0.15 eV.

3.1.3. High Field Conduction

For field strengths greater than 0.3 mV/cm, the high field characteristic was always of the form;

$$I \alpha \exp (\beta V^{\frac{1}{2}})/kT. \quad (1)$$

This is the same form as already observed by previous workers [3-5, 7, 8]. A set of curves at different temperatures is shown in fig. 4. The Poole-Frenkel form of equation 1 is

$$I \alpha \exp (\beta_{\mathrm{pf}} V^{\frac{1}{2}} - \phi)/kT \quad (2)$$

where

$$\beta_{\mathrm{pf}} = [(e^3/4\pi \epsilon'_{\mathrm{pf}} \epsilon_0 d)^{\frac{1}{2}}] \quad (3)$$

ϕ represents the energy depth of a trap, e is the electronic charge and d the film thickness.

Although breakdowns occurred at fields in excess of 2 mV/cm, the changes in the characteristic were not sufficient to disallow determination of ϕ and ϵ'_{pf}. The value of ϕ was 0.55 ± 0.05 eV and the permittivity $\epsilon'_{\mathrm{pf}} \simeq 11$. The Schottky emission form of equation 2 is similar but with $\beta_{\mathrm{se}} = \beta_{\mathrm{pf}}/2$ so that $\epsilon'_{\mathrm{se}} = e'_{\mathrm{pf}}/4$. This gives a value of permittivity of $\simeq 2.7$.

Above 2 mV/cm the breakdowns which occurred were generally of the propagating variety.

3.2. AC Conduction

The frequency range which received the most detailed attention was 300 c/s to 15 kc/s. The frequency range 30 kc/s to 1 mc/s was investigated and it was found that both loss and permittivity were independent of frequency up to the highest temperature of measurement (about 200° C).

For identical deposition conditions and heat-treatment, a range of loss tangents of about two orders of magnitude from 0.02 to 2% were observed at room temperature. The form of the loss tangents as functions of frequency and temperature were similar, however, and fig. 5 illustrates the loss as a function of frequency at constant temperatures. The slope of the straight line portion of these curves is denoted by $-\gamma(T)$. A second method of observing the loss is to plot conductance as a function of frequency as shown in fig. 6. The slope of the straight line portion is denoted by $\alpha(T)$. Since the change in capacitance is small compared to the change in conductivity, then $\alpha(T) = 1 - \gamma(T)$ and a plot of this function as a function of temperature is shown in fig. 7. For temperatures below 80° C, $\alpha(T)$ has a value of 0.8. At higher temperatures $\alpha(T)$ falls but appears to flatten off at about 0.3 ± 0.1, above 200° C.

Fig. 8, of conductance versus reciprocal

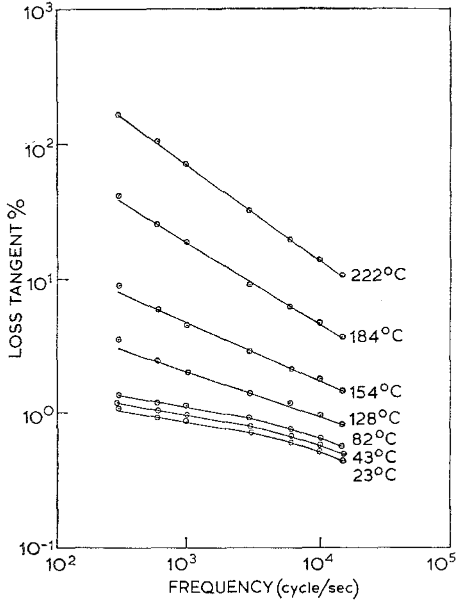

Figure 5 Loss tangent versus frequency at constant temperatures.

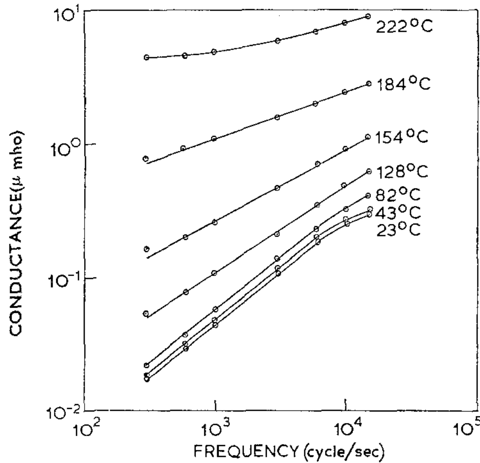

Figure 6 Conductance versus frequency at constant temperatures.

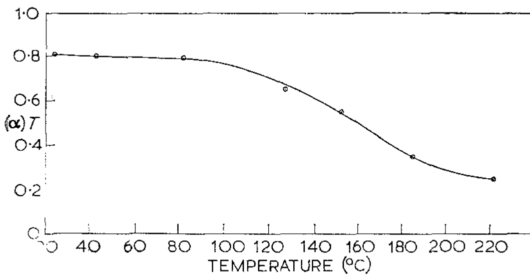

Figure 7 The function, $\alpha(T) = 1 - \gamma(T)$, versus temperature.

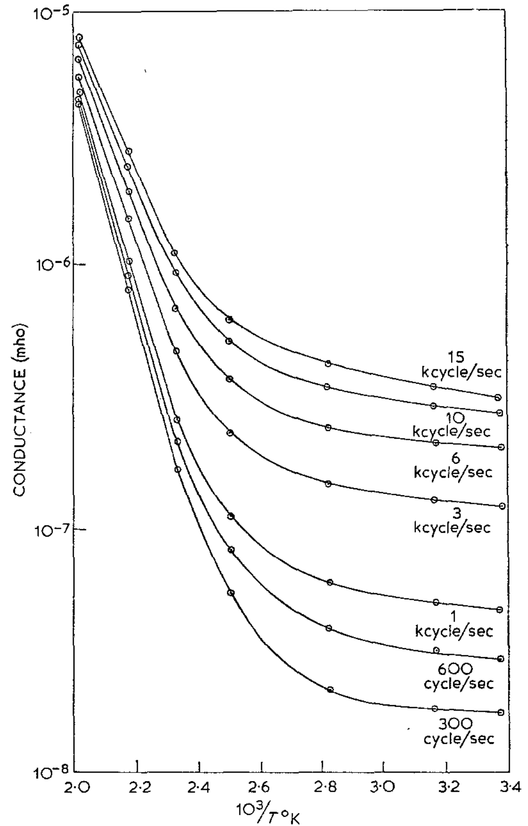

Figure 8 Conductance versus reciprocal temperature.

temperature, suggests that the frequency range considered represents a transition region between two conduction processes. The low-temperature activation energy does not appear to have reached a constant value but will be less than 0.1 eV. The slope of the high-temperature region suggests an activation energy of 0.8 eV. However, it is necessary to look at the equations involved in AC conduction theory before we can define an activation energy, particularly when a distribution of relaxation times is involved. A convenient method of describing AC loss in a dielectric is the Cole-Cole [14] form of the Debye equations. The Cole-Cole equations describe all situations from a single relaxation time process to an infinite distribution of relaxation times. The complex permittivity ϵ^* for the Cole-Cole distribution is,

$$(\epsilon^* - \epsilon_\infty)/(\epsilon_s - \epsilon_\infty) = 1/[1 + (j\omega\tau_0)^{1-\beta}] \quad (4)$$

where ϵ_s and ϵ_∞ are the static and high frequency limits of the real part of the permittivity, τ_0 is the mean or most probable relaxation time and represents the width of the distribution of

relaxation times. ϵ^* can be split into its real and imaginary components ($\epsilon^* = \epsilon' - j\epsilon''$), and for frequencies greater than the relaxation frequency ($\omega_0 = 1/\tau_0$), the following approximation can be made for the conductivity, σ,

$$\sigma = \omega\epsilon_0\epsilon'' \simeq \frac{\epsilon_0 (\epsilon_s - \epsilon_\infty)\,\omega}{(\omega\tau_0)^{1-\beta}} \simeq \frac{\epsilon_0 (\epsilon_s - \epsilon_\infty)\,\omega^\beta}{\tau_0^{1-\beta}}$$

where ϵ_0 is the permittivity of free space in mks units. For a very broad distribution of relaxation times, $\beta \to 1$, and the loss tangent ($\tan\delta = \epsilon''/\epsilon'$) becomes independent of frequency.

The absorption current measurements indicated a low-frequency relaxation peak and it is suggested that at high temperatures it is the tail of this peak which is producing the dispersion in loss at low frequencies. If we describe the relaxation mechanism by a Cole-Cole distribution and assume that this dispersion dominates other forms of conduction at the highest temperatures of measurement then we can equate the limiting value of $\alpha(T)$ to $\beta \simeq 0.3$.

This is discussed further in section 4.2.3. By relating τ_0 to the temperature by the Arrhenius relationship $\tau_0 = \tau_\infty \exp E/kT$, we obtain the following form for the conductance G

$$G \propto \exp\left[\{-(1-\beta)\,E\}/kT\right]$$

Thus the activation energy E is given by $0.8/1-\beta \simeq 1.0 \pm 0.1$ eV.

4. Discussion

4.1. Absorption Current

The time dependent current has been related to a low-frequency loss mechanism occurring in the region 5×10^{-3} c/s. Hamon [9] quoted a maximum error of $\pm 15\%$ for his analysis provided that the value of n defining a linear dielectric ($I \propto t^{-n}$) was in the range $0.3 < n < 1.2$. Experimentally n was found to depart from this range. However, Baird [15] showed that if the relaxation mechanism could be described by a Cole-Cole [14] distribution, then the equation defining a linear dielectric could not possibly hold for all values of time t. Williams [16] showed that for frequencies within $\pm$ 0.01 of the relaxation frequency $1/2\pi\tau_0$ c/s, the Hamon equation was reasonably accurate. The only information obtained in this case is that there is a low frequency loss mechanism in the region 5×10^{-3} c/s. Low-frequency dispersions are usually associated with interfacial polarisation effects and it is suggested that this is the case for silicon oxide. Hirose and Wada [2] suggested that the migrating ion was free silicon but it is thought that for the deposition conditions used in this case, the existence of free silicon is unlikely. The work of glass technologists suggests that the ionic species responsible for this effect are probably those of the alkaline metals, but further than this, it is not possible to make a more detailed analysis. Argall suggested that his low-frequency type B relaxation peak was an interfacial effect. However there is not sufficient information in this work to differentiate between different mechanisms.

4.2. DC Conduction

4.2.1. Low Field Conduction

There are two known conduction mechanisms which result in an ohmic characteristic. These are ionic conduction and impurity conduction and are discussed in detail by Lamb [17]. However, due to the range of conductivities which were found experimentally it is suspected that the low field conduction is controlled by weak paths in the material as suggested by Siddall [1]. The actual mechanism of current flow in these flaws is not yet understood.

4.2.2. High Field Conduction

The results for high field conduction agree reasonably well with those of previous authors. As discussed by Jonscher [10] these results do not fit exactly either the models of Schottky emission or Poole-Frenkel conduction but we cannot, therefore, dismiss these models. Jonscher [10] investigated the assumptions which were made in the derivation of the Poole-Frenkel equation. He showed that certain modifications would produce a model which gave better agreement with experimental results for silicon oxide.

The amorphous nature of dielectric materials probably introduces localised sites within the forbidden band. The nature of these sites has been discussed by Gubanon [18] and Mott [19] and their existence is still a matter of some uncertainty. These sites would act as trapping centres and the activation energy of 0.55 eV would then represent the energy required to excite an electron from such a site into the insulator conduction band. However, the energy band structure suggested by Jonscher [10] gives no well defined conduction band edge but a quasi-continuum of localised levels thus making it difficult to give a precise interpretation of the activation energy.

4.2.3. AC Conduction
As suggested previously, the audio-frequency region represents a transition beween two conduction processes. The high-temperature region, particularly at low frequencies, is dominated by the low-frequency dispersion predicted by the DC absorption current. The high-temperature limit of $\alpha(T)$, then corresponds to β as defined by the Cole-Cole plot (equation 1) and has a numerical value of 0.3 ± 0.1 (Taylor [20] and Owen and Douglas [21] working on silicate glasses found β to be independent of temperature). This implies that there will be a small distribution of relaxation times. The most probable activation energy represents a barrier height over which a migrating ion must be excited during its travel.

At room temperature the region was being approached where loss was independent of frequency, i.e. $\sigma\alpha\omega$. The limit reached in the audio-frequency case was $\sigma\alpha\omega^{0.8}$. This high-frequency region has a conduction mechanism with a very broad distribution of relaxation times. It is not possible to give an exact activation energy but it will be less than 0.1 eV. Such a low activation energy will almost certainly be associated with an electronic process. It is suggested that an electron hopping mechanism explains the above behaviour. This mechanism was suggested by Pollack and Geballe [22] to explain their experimental results ($\sigma\alpha\omega^{0.8}$) in doped semi-conductors at temperatures near absolute zero. In an amorphous dielectric at room temperature the hopping sites would probably be the localised sites in the forbidden band. At one particular frequency only a small number of pairs of sites will contribute to the loss with a particular spatial and energy separation. It is expected that there will be a distribution of these separations due to the amorphous structure. Pollack and Geballe [22] and Miller and Abrahams [23] showed that the relaxation time associated with a particular spatial separation was an experimental function of that separation. A very broad distribution of relaxation times would be expected, therefore, for such a mechanism.

Conclusion
Four activation energies have been determined for conduction processes in films of silicon oxide. These are summarised in table III, together with the suggested modes of conduction.

References

1. G. SIDDALL, *Vacuum* **9** (1959) 274.
2. H. HIROSE and Y. WADA, *Jap. J. Appl. Phys.* **3** (1965) 179.
3. *Idem, ibid* **4** (1965) 636.
4. I. T. JOHANSEN, *J. Appl. Phys.* **37** (1966) 2.
5. T. E. HARTMAN, J. C. BLAIR, and R. BAUER, *ibid* **37** (1966) 6.
6. F. ARGALL, Ph.D. thesis, Chelsea College, London University (1968).
7. M. STUART, *Brit. J. Appl. Phys.* **18** (1967) 1637.
8. *Idem, Phys. Status Solidi.* **23** (1967) 595.
9. D. V. HAMON, *Proc. I.E.E.* **99** (1952) 115.
10. A. K. JONSCHER, *Thin Solid Films* **1** (1967) 213.
11. J. G. SIMMONS, *Phys. Rev.* **155** (1967) 657.
12. A. R. MORLEY and D. S. CAMPBELL, *Thin Solid Films* **2** (1969) 403.
13. C. E. DRUMHELLER, Trans. 7th Nat. Vac. Symp., edited by C. R. Maissel, (Pergamon, New York, 1961).
14. K. S. COLE and R. H. COLE, *J. Chem. Phys.* **9** (1941) 341.
15. M. E. BAIRD, *Rev. Mod. Phys.* **40** (1968) 219.
16. G. WILLIAMS, *Trans. Faraday Soc.* **58** (1962) 1041.
17. D. R. LAMB, "Electrical Conduction Mechanisms In Thin Insulating Films" (Methuen, London, 1967).
18. A. I. GUBANON, "Quantum Electron Theory of Amorphous Conductors" Consultants Bureau, New York, 1965).
19. N. F. MOTT, *Adv. Phys.* **16** (1967) 49.
20. H. E. TAYLOR, Ph.D. thesis, University of Sheffield (1954).
21. A. E. OWEN and R. W. DOUGLAS, *J. Soc. Glass Tech.* **43** (1952) 159T.
22. M. POLLACK and T. H. GEBALLE, *Phys. Rev.* **122** (1961) 1742.
23. A. MILLER and E. ABRAHAMS, *ibid* **120** (1960) 745.
24. J. J. O'DWYER, *Bull. Amer. Phys. Soc.* **10** 1965 189; *J. Appl. Phys.* **37** (1966) 599.

TABLE III Summary of activation energies in Si—O.

		Activation energy	Suggested process
DC conduction	Low field	0.7 ± 0.15 eV	Weak path conduction
	High field	0.55 ± 0.05 eV	Modified Poole-Frenkel as suggested by Jonscher [10]
AC conduction	Low frequency	1.0 ± 0.1 eV	Interfacial polarisation with blocking electrodes
	High frequency	< 0.1 eV	Electron hopping mechanism